East European Journal of Physics. 1. 45–59 (2026)
DOI: 10.26565/2312-4334-2026-1-04 ISSN 2312-4334

COSMOLOGICAL DYNAMICS OF TSALLIS HOLOGRAPHIC DARK ENERGY IN SAEZ-BALLESTER GRAVITY

P.E. Satyanarayana, K.V.S. Sireesha*, K.P.S. Suryanarayana, R. Sathibabu
Department of Mathematics, GSS, GITAM Deemed to be University, Visakhapatnam, India
Corresponding Author e-mail: sireeshakuppili@gmail.com
Received December 19, 2025; revised February 3, 2026; accepted February 10, 2026

- The cosmological models of Tsallis holographic dark energy (THDE) are examined within the framework of Sáez–Ballester (SB) gravity.
- Bianchi type II, VIII, and IX anisotropic universes with the Hubble horizon cutoff were analysed.
- Models extend beyond ΛCDM, predicting continuous acceleration and phantom-like behaviour ($w < -1$)
- he natural transition from the dominance of early matter to the dominance of late dark energy is reconstructed.
- Anisotropy diminishes over time, facilitating isotropization in accordance with CMB findings.
- Entropy modifications are more important than geometric differences, which shows that THDE is strong across anisotropic backgrounds.

We investigate interacting and non-interacting Tsallis Holographic Dark Energy (THDE) models within the framework of Sáez–Ballester (SB) scalar–tensor gravity for anisotropic Bianchi type(BT) II, VIII, and IX Universes. Employing the Hubble horizon as the infrared cutoff, we examine the models without assuming a particular scale factor law. The analysis covers key cosmological parameters, including the deceleration parameter, Hubble parameter, energy densities, skewness, the Equation of State (EoS), and the Squared sound speed. Our findings indicate a continuous phantom-like acceleration ($w < -1$) with transition redshift $z_t \approx 0.67$ and negligible late-time anisotropy, consistent with cosmic microwave background (CMB) bounds. Compared to ΛCDM, the THDE models predict an earlier onset of acceleration and a more negative present-day EoS. However, the presence of negative squared sound speed at higher redshifts signals a classical instability of the dark energy fluid. These results highlight THDE as a viable alternative to ΛCDM in anisotropic cosmologies, while motivating further work with alternative cutoffs or stabilising mechanisms to overcome the instability issue.

Keywords: *BT-II; VIII & IX models; Tsallis Holographic Dark Energy; Saez-Ballester theory of gravity; Cosmic acceleration; Anisotropic cosmology*

PACS: 95:30.sf, 95.35+d ,95.36+x
MSC: 85-xx, 85-08, 85A40, 85A99

1. INTRODUCTION

The understanding of the Universe has expanded significantly in recent years. It is widely assumed that around 95% of our Universe is made up of two unknown components known as dark matter (DM) and dark energy (DE). These two components generate fundamental issues and imply that fundamentally new physics should be investigated. DM constitutes approximately 25% of the Universe's total energy density (ED). While astrophysical studies on various scales have established the presence of DM, its nature remains unclear.DE is an unexplored component of our cosmos. Dark energy, distinct from ordinary baryonic matter due to its strong negative pressure, drives the Universe's expansion and constitutes over 70% of its energy density. While Einstein's cosmological constant could represent the dark energy model, its required magnitude challenges our understanding of its quantum characteristics. Unknown changes in dynamical fields or changes in General Relativity might induce DE. Cosmic microwave background (CMB) anisotropies, large-scale structure, and type-Ia supernovae are some of the cosmological advancements that allow the cosmos to expand more quickly. DE, an unexpected fluid with negative pressure, is the source of this accelerated phase. There are two explanations for the Universe's late-time acceleration. Einstein's field equations may be modified to generate dynamic DE models by modifying the matter component. Despite issues with cosmic coincidence and fine-tuning, the cosmological constant remains the most viable candidate for explaining DE. Numerous dark energy (DE) theories have been formulated to address these issues, including quintessence [1],tachyon[2],ghost [3], k-essence[4], f-essence [5, 6], phantom [7], Chaplygin gas[8], holographic dark energy (HDE) [9, 10, 11], and new-age graphic dark energy (NADE)[12, 13]. Integrating Dark Energy with Dark Matter may alleviate the cosmic coincidence problem. On the other hand, many modified gravity theories, such as f (R) theory[14],

Cite as: P.E. Satyanarayana, K.V.S. Sireesha, K.P.S. Suryanarayana, R. Sathibabu, East Eur. J. Phys. 1, 45 (2026), https://doi.org/10.26565/2312-4334-2026-1-04
© P.E. Satyanarayana, K.V.S. Sireesha, K.P.S. Suryanarayana, R. Sathibabu, 2026; CC BY 4.0 license

f (T) theory[15], Horava-Lifshitz gravity [16, 17, 18, 19], Brans-Dicke theory [20], Gauss-Bonnet theory[21] , and f (R, T) theory [22], have been created by modifying the geometric component of the Einstein gravitational field equations. SB[23] scalar–tensor theory is a well-studied alternative to general relativity in which gravity is mediated by both the metric and a dimensionless scalar field ϕ. In this theory, the scalar field couples nontrivially to geometry while remaining dimensionless — a feature that allows for novel cosmological dynamics without the introduction of an explicit potential term. The theory has been widely applied to homogeneous and anisotropic cosmologies and has proved useful in modelling late-time acceleration, viscous fluids, and higher-dimensional cosmologies. In parallel, HDE models based on generalized (non-additive) entropy formalisms — in particular THDE have attracted attention as phenomenological alternatives to the standard cosmological constant, since the Tsallis entropy introduces a parameter that effectively modifies the DE equation of state and the cosmic evolution. Recently, several authors have combined THDE with SB gravity and investigated the cosmological consequences in FRW, Kaluza–Klein and anisotropic Bianchi backgrounds, deriving reconstruction schemes, stability/thermodynamic analyses, and interacting/non-interacting scenarios; these studies indicate that THDE in the SB framework can produce viable late-time acceleration and a rich dynamical behaviour that depends sensitively on the Tsallis parameter and the SB scalar-field coupling. For instance, Santhi and Babu[24] studied a BT-III THDE model in SB theory, showing its consistency with an accelerating universe. Dheepika and Mathew[25] reconsidered THDE models in SB gravity with improved stability analysis. Dasunaidu et al.[26] examined the Kaluza–Klein FRW THDE model and discussed the role of higher dimensions in cosmic evolution. Rao et al. [27] investigated anisotropic Sharma–Mittal HDE in SB theory, while Murali et al. [28] employed a cosmographic analysis of an anisotropic Kaniadakis HDE model, demonstrating the versatility of generalized holographic dark energy models in the SB framework. Collectively, these works highlight that SB theory, when combined with entropy-based dark energy formalisms, can successfully reproduce the evolution from slowdown to rapid acceleration, offering viable alternatives to ΛCDM. In parallel, anisotropic cosmological models, particularly BT spacetimes, provide a natural generalization of the standard FLRW universe and are especially relevant for probing the early universe, where isotropy may not yet have been established. Bianchi cosmologies are spatially homogeneous but anisotropic models classified into nine types (I–IX) according to the structure of their three-dimensional Lie groups of isometries. By allowing distinct scale factors in different spatial directions, they extend the isotropic FRW framework and offer a useful platform for studying the role of anisotropies in cosmic evolution, structure formation, and modified gravity theories. Among these, BT-II, VIII, and IX are of particular interest because they admit richer geometric structures and more complex dynamical anisotropy evolution. Embedding DE models in such anisotropic backgrounds has been shown to produce distinctive signatures in cosmic expansion, thereby providing a means to probe the role of anisotropies in the early universe. Santhi et al. [29] analysed viscous HDE theories of cosmology within the Brans–Dicke framework, whereas in SB gravity, bulk viscous string cosmological models were discussed by Rao et al. [30]. Sireesha and Rao [31, 32] contributed further by analyzing BT-II, VIII, and IX holographic dark energy models in Brans–Dicke theory, as well as modified holographic Ricci dark energy scenarios in f (R,T) gravity.More recently, Wath & Nimkar [33] investigated BT-VIII configurations in the SB framework, incorporating anisotropic dark matter and analyzing their stability and energy conditions. In order to prevent black hole creation in quantum field theory, the vacuum energy of a system of size 'L' must not be more than the mass of a black hole of the same size. This principle is used to develop the HDE model within quantum gravity. In the holographic dark energy framework, the energy density is expressed in terms of the infrared (IR) cutoff scale as

$$\rho_t = 3c^2 m_p^2 L^{-2} \tag{1}$$

Where m_p^2 represents the reduced Planck mass, the quantum field's vacuum energy density is measured against several kinds of cutoffs, including ultraviolet and infrared. Granda and Oliveros [34] introduced an infrared (IR) cutoff based on local Hubble quantities and their time derivatives. The advantages of this new HDE model, using the Granda and Oliveros cutoff, include its reliance on local quantities, avoidance of causality issues associated with the event horizon infrared cutoff, and its ability to describe the Universe's accelerated expansion. Additionally, it confirms that the evolution from a decelerating period to an accelerating period is consistent with existing data from observations [34]. Recently, the HDE model has gained interest for its ability to explain the constant ratio between DM and DE densities in the present Universe. Studies also suggest that the HDE model aligns well with observational data. Recent studies have employed various entropy formalisms to investigate gravitational and cosmological phenomena. Notably, HDE models have been examined through frameworks like THDE [35], RHDE [36], and SMHDE [37] . Sharif and Jawad [38] examined the cosmic development of interacting non-flat NHDE. Li et al. [39] employed Planck data to explore the cosmic implications of the HDE scenario. The cosmology and thermodynamics of the HDE model were examined by Praseetha and Mathew [40], who analysed the generalised second law of thermodynamics in a flat universe with interactions between DE and DM. Jawad et al.[41] conducted a study on the thermodynamic consequences of a modified HRDE model, focusing on the interaction between its energy density and that of CDM is examined under the context of Chameleon Brans-Dicke gravity. For this study, we use the HDE model with a modified entropy formalism, which is called Tsallis HDE, to reach the objective. Dubey et al. [42] examined THDE models within axially symmetric BT-I space-time, utilising the Hubble horizon as the infrared cutoff. In contrast, Dubey et al.[43] investigated THDE within a BT-I Universe, employing a hybrid expansion law in conjunction with k-essence. To date, no studies have explored the THDE model with an anisotropic background in the SB scalar-tensor theory of gravity. As a result, we investigated the dynamics of THDE in BT-II, VIII, and IX space-times using the Hubble horizon as the infrared cutoff and the SB gravity theory. Without assuming anything about the average

scale factor's expansion rule, By calculating the field equations of our proposed THDE model, we found an exact and suitable response. Aditya and Reddy suggested an anisotropic new HDE model inside the SB theory of gravity [44] . Prasanthi and Aditya[45] studied anisotropic RHDE models using general relativity as a framework. Gravitational and cosmic events have been studied using several entropy formalisms in the last few years. Tsallis generalised entropy-based THDE is intrinsically unstable at the classical level [46, 47]. Within the logarithmic Brans-Dicke (BD) theory framework, Aditya et al. [48] investigated observational limitations on interacting THDE. Two recent studies have investigated several models of THDE: Pandey et al. [49] and Kumar et al. [50], which focused on the quintessence model.

The combination of THDE, SB theory, and anisotropic Bianchi space-times thus provides a well-motivated framework to address outstanding questions about cosmic acceleration, the role of anisotropies, and deviations from Λ CDM. In particular, it enables the investigation of how generalized entropy corrections and scalar–tensor couplings influence the stability, energy conditions, and observational viability of anisotropic cosmological models. In BT-II, VIII, and IX space-times under SB gravity, with the Hubble horizon as the infrared cutoff, this study gives the field equations for interacting and non-interacting THDE models, as well as their solutions. We study the time-dependent changes in important physical characteristics and evaluate their stability in terms of the squared speed of sound, drawing qualitative comparisons to the expected general behaviour in classic Λ CDM cosmology. The study aims to evaluate whether THDE in SB theory can serve as a viable alternative to Λ CDM in anisotropic cosmologies and to explore the cosmic evolution in the initial and late universes as a result of anisotropies. Here, we take a look at the THDE models via an understanding of SB theory.

THDE is based on the non-extensive entropy formalism and provides a standard structure in which the infrared cutoff and the non-extensive parameter determine how dark energy evolves, allowing it to behave like a phantom or quintessence. The SB theory, although mathematically equivalent to general relativity with a minimally associated scalar field resulting in a field reorganization, has been extensively utilized in anisotropic contexts due to its straightforward scalar–tensor configuration and analytical manageability. In this study, THDE serves as the dynamic control of late-time acceleration, whereas the SB scalar primarily impacts early-time dynamics. This combination allows us to observe how generalised holographic dark energy evolves in anisotropic configurations and how quickly these kinds of universes become isotropic, which is the conventional ΛCDM limit.

This study is organised as follows. Section 2 formulates the field equations of SB theory, incorporating THDE and pressureless DM. Section 3 develops both non-interacting and interacting THDE cosmological models and presents their physical analysis. Section 4 outlines the key findings, observational consistency, and comparisons with the standard ΛCDM scenario. Finally, Section 5 provides a detailed discussion and conclusion, highlighting the model's implications, limitations, and prospects.

2. FIELD EQUATIONS IN SAEZ-BALLESTER'S THEORY OF GRAVITY

There have been studies of THDE in other Bianchi and scalar–tensor frameworks before, but this is the first time that the combined study of interacting and non-interacting THDE in SB gravity for the BT-II, VIII, and IX geometries with accurate analytical solutions has been addressed in depth. Previous studies predominantly concentrated on Bianchi I or III backgrounds, or on specific selections of scale components. Conversely, this study establishes the complete field equations for these three anisotropic categories, derives exact solutions based on consistent parameter relations, and examines the dynamical quantities, including the equation of state, deceleration parameter, evolution of anisotropy, and stability. This offers a more integrated and methodical analysis of THDE conduct across various anisotropic geometries. We take into account the spatially homogenous BT-II, VIII and IX metrics of the form.

$$ds^2 = dt^2 - R^2\left[d\theta^2 + f^2(\theta)\, d\phi^2\right] - S^2\left[d\psi + h(\theta)\, d\phi\right]^2 \tag{2}$$

This is when the Eulerian angles (θ, ϕ, ψ) and the functions R and S are defined exclusively with respect to 't'. When the values of $f(\theta) = 1, Cosh\theta$ & $Sin\theta$ and $h(\theta) = \theta, Sinh\theta$ & $Cos\theta$, then it represents BT -II, VIII & IX respectively.
It is essential to make clear that, employing the field modification, the SB theory under consideration is dynamically equivalent to general relativity with a minimally coupled massless scalar field $\phi = \frac{2}{n+2}\sqrt{\omega}\,\phi^{\frac{n+2}{2}}$. The scalar field effectively behaves as a stiff fluid with $\rho_\phi \propto a^{-6}$ under this mapping, and the SB action corresponds to that of an Einstein–massless–scalar (EMS) system. As a result, late-time acceleration is not possible with the SB scalar, since it disintegrates significantly more rapidly than radiation. The SB field primarily contributes to early-epoch dynamics in our model, whereas the Tsallis holographic dark energy component is the only source of the rapid expansion. By addressing the SB framework's fundamental shortcomings, this clarification strengthens the theoretical foundation for our findings. In place of Einstein's general theory of gravity, a number of gravitational theories have been proposed. Despite this, BD scalar-tensor theory is still regarded as the best substitute for the theory of Einstein. This study investigates a Universe characterised by pressure-less dark matter, with energy density ρ_m, and dark energy with density ρ_t. Consequently, utilising geometrised units 8πG =C= 1, the SB field equations for the combined scalar and tenor fields are given here by

$$G_{ij} - \omega\phi^m\left(\phi_{,i}\phi_{,j} - \frac{1}{2}g_{ij}\,\phi_{,k}\phi^{'k}\right) = -\left(T_{ij} + \bar{T}_{ij}\right) \tag{3}$$

When the scalar field meets the requirements of the equation

$$2\phi^m \phi^i{}_{,j} + m\phi^{m-1}\phi_{,k}\phi'^k = 0 \tag{4}$$

Where $G_{ij} = R_{ij} - \frac{1}{2}Rg_{ij}$ is an Einstein tensor, R is the scalar curvature, ω and m are constants, and $T_{ij} + \bar{T}_{ij}$ represents the stress-energy tensor associated with the matter and DE. We have an energy conservation equation as

$$\left(T_{ij} + \bar{T}_{ij}\right)_{;j} = 0 \tag{5}$$

The THDE energy-momentum tensor $\bar{T}_{ij}$ is structured here:

$$\bar{T}_{ij} = (\rho_t + p_t)u_i u_j - p_t g_{ij} = \text{diag}\left[1, -w_t, -w_t, -w_t\right]\rho_t \tag{6}$$

It can be parameterized as

$$\bar{T}_{ij} = \text{diag}\left[1, -w_t, -w_t, -(w_t + \gamma)\right]\rho_t \tag{7}$$

In this context, ρ_t, ρ_m represent the energy densities of THDE and matter, respectively, while p_t denotes the pressure of THDE. The equation of state (EoS) parameter is defined as $w_t = \frac{p_t}{\rho_t}$. Here, γ represents the deviation from the EoS parameter in the ψ-direction, referred to as the skewness parameter. Using Equations (6)-(7), the SB field equations for BT-II, VIII and IX Universes (2) can be expressed as follows.

$$\frac{\ddot{R}}{R} + \frac{\ddot{S}}{S} + \frac{\dot{R}\dot{S}}{RS} + \frac{S^2}{4R^4} - \frac{\omega}{2}\phi^m\dot{\phi}^2 = -w_t\rho_t \tag{8}$$

$$2\frac{\ddot{R}}{R} + \frac{\dot{R}^2 + \vartheta}{R^2} - \frac{3S^2}{4R^4} - \frac{\omega}{2}\phi^m\dot{\phi}^2 = -(w_t + \gamma)\rho_t \tag{9}$$

$$2\frac{\dot{R}\dot{S}}{RS} + \frac{\dot{R}^2 + \vartheta}{R^2} - \frac{S^2}{4R^4} + \frac{\omega}{2}\phi^m\dot{\phi}^2 = \rho_m + \rho_t \tag{10}$$

$$\ddot{\phi} + \dot{\phi}\left(2\frac{\dot{R}}{R} + \frac{\dot{S}}{S}\right) + \frac{m\dot{\phi}^2}{2\phi} = 0 \tag{11}$$

$$\dot{\rho}_m + \dot{\rho}_t + \left(2\frac{\dot{R}}{R} + \frac{\dot{S}}{S}\right)(\rho_m + (1 + w_t)\rho_t) + \gamma\frac{\dot{S}}{S}\rho_t = 0 \tag{12}$$

When $\vartheta = 0, -1\ \&1$, the cosmological models correspond to BT-II, VIII and IX, respectively.

3. THDE COSMOLOGICAL MODELS

The standard cosmological model depends on isotropy; however, anisotropic Bianchi universes function as significant theoretical frameworks for examining the durability of dark-energy models, the methodology for achieving isotropy, and initial departures from the FLRW baseline. Current Planck CMB observations only limit the present-day shear to be very minimal; they do not rule out the existence of anisotropies in older epochs. Bianchi models enable the investigation of whether THDE dynamics fundamentally accelerate the Universe towards isotropy in later epochs, a crucial criterion for alignment with observations.

By addressing the nonlinear field equations with certain physically reasonable assumptions, we develop THDE cosmological models. To achieve a deterministic solution, we rely on the following physically plausible condition:

- The shear scalar σ^2 is proportional to the scalar expansion θ, establishing a relationship between the metric potentials.

$$S = R^n \tag{13}$$

From equations (8),(9)and (13), we get

$$\frac{\ddot{R}}{R} + (1 + n)\frac{\dot{R}^2}{R^2} + \frac{\vartheta}{(1 - n)R^2} - \frac{R^{2n-4}}{1 - n} = \frac{\gamma\rho_t}{n - 1}, \qquad n \neq 1 \tag{14}$$

To solve Equation (14) , we adopt the following physically reasonable assumption.

$$\gamma = \frac{\gamma_0(n - 1)}{\rho_t} \text{ for BT-II model} \tag{15}$$

$$\gamma = \frac{\gamma_0(n - 1)R^2 + 1}{\rho_t R^2} \text{ for BT-VIII model} \tag{16}$$

$$\gamma = \frac{\gamma_0(n - 1)R^2 - 1}{\rho_t R^2} \text{ for BT-IX model} \tag{17}$$

Where γ_0 is an arbitrary constant. from equations (14) & (15), we get the metric potentials

$$R = \left[\frac{C_1}{C_2}\,\mathrm{sech}(C_1(2-n)t)\right]^{\frac{1}{n-2}} \tag{18}$$

$$S = \left[\frac{C_1}{C_2}\,\mathrm{sech}(C_1(2-n)t)\right]^{\frac{n}{n-2}} \tag{19}$$

Where $C_1^2 = \frac{\gamma_0}{2(n+2)}$ and $C_2^2 = \frac{1}{4n(n-1)}$. Substituting the values of R and S in Equations (18)and (19), we find that the scalar field.

$$\phi^{\frac{m+2}{2}} = \left(\frac{m+2}{2}\right)\left\{C\left(\frac{C_2}{C_1}\right)^{\frac{n+2}{n-2}}\int\left[\cosh\left(C_1(2-n)t\right)\right]^{\frac{n+2}{n-2}}\,dt\right\} \tag{20}$$

Where C is constant. Using the metric potentials (18) and (19) in the metric (2), we can write

$$\begin{aligned} ds^2 = dt^2 &- \left[\frac{C_1}{C_2}\,\mathrm{sech}(C_1(2-n)t)\right]^{\frac{2}{n-2}}\left[d\theta^2 + f^2(\theta)\,d\phi^2\right] \\ &- \left[\frac{C_1}{C_2}\,\mathrm{sech}(C_1(2-n)t)\right]^{\frac{2n}{n-2}}\left[d\psi + h(\theta)\,d\phi\right]^2 \end{aligned} \tag{21}$$

Equation (20) specifies the BT-II, VIII and IX THDE cosmological models in the SB scalar-tensor theory of gravity, as well as the following properties:

1. In anisotropic geometries, different spatial directions expand at distinct rates, which may lead to direction-dependent observational effects such as anisotropic redshifts.
2. The global expansion of the universe is characterized by the average scale factor $a(t) = (ABC)^{\frac{1}{3}}$, which allows us to derive analytical expressions and investigate the overall dynamical behavior of the model.
3. A detailed confrontation with observational data would require a direction-dependent analysis of luminosity distance and Hubble flow, which lies beyond the scope of the present work and is left for future investigation.

With the anisotropic framework and average expansion established, we now investigate the physical properties of the model, including the spatial volume, expansion scalar, shear scalar, anisotropy parameter, Hubble parameters, and the deceleration parameter, which together characterize the dynamical behavior of the universe.
The volume of space is

$$V = R^2S = \left[\frac{C_1}{C_2}\,\mathrm{sech}\big(C_1(2-n)t\big)\right]^{\frac{n+2}{n-2}} \tag{22}$$

The scale factor, on average, is

$$a(t) = V^{\frac{1}{3}} = \left[\frac{C_1}{C_2}\,\mathrm{sech}\big(C_1(2-n)t\big)\right]^{\frac{n+2}{3(n-2)}} \tag{23}$$

The scalar equations for expansion and shear are

$$\begin{aligned} \theta = 3H &= (n+2)C_1\tanh\left(C_1(2-n)t\right) \\ \sigma^2 &= \frac{7}{18}\theta^2 = \frac{7}{18}\left[(n+2)C_1\tanh\left(C_1(2-n)t\right)\right]^2 \end{aligned} \tag{24}$$

The deceleration parameter for our model is provided by

$$q = -\frac{3\dot{\theta}}{\theta^2} - 1 = \frac{n-2}{n+2}cosech^2\big(C_1(2-n)t\big) - 1 \tag{25}$$

The graph presents the deceleration parameter versus redshift in the framework of THDE, showcasing a persistent and intensifying cosmic acceleration. Covering a redshift range of $z = 2.5$ to $z = -1$, the curve remains negative throughout, indicating that the Universe is in a continuous accelerated expansion phase. Notably, as z increases beyond approximately 2, the deceleration parameter sharply drops to tremendous negative values, reflecting an intense acceleration in the early Universe. As a result, the THDE framework predicts a dominant and phantom-like DE influence even in the early Universe. The absence of any transition to a decelerating phase, as seen in standard models like Λ CDM, underlines the non-trivial role of THDE in cosmic dynamics and establishes it as a compelling candidate to explain the Universe's super-accelerated expansion throughout its history, especially within anisotropic cosmological backgrounds. However, the super-exponential expansion ($q < -1$) would indicate that the rate of acceleration in the Tsallis model is more rapid or intense than the Λ CDM model.

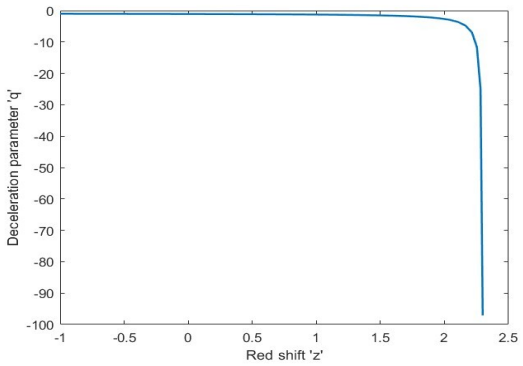

Figure 1. Deceleration parameter plotted against redshift for the SB cosmology for $\gamma_0 = 6.5$ & $n = 1.5$.

For our model, the Hubble parameter(H) can be obtained as

$$H = \frac{(n+2)C_1}{3} \tanh\left(C_1(2-n)t\right) \tag{26}$$

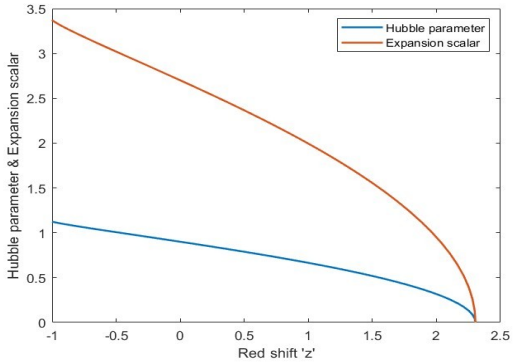

Figure 2. Hubble parameter and the Expansion scalar are plotted against redshift for the SB cosmology for $\gamma_0 = 6.5$ & $n = 1.5$.

The graph depicting the Hubble parameter and expansion scalar versus redshift in the THDE framework reveals crucial insights into the Universe's dynamic evolution. These two critical observable cosmological elements are essential to the Universe's expansion rate. The Hubble parameter and the expansion scalar graphs demonstrate that they are positive-valued accelerating cosmic time functions over extended periods. As redshift increases, both the Hubble parameter (H) and expansion scalar (θ) exhibit a monotonically decreasing trend, indicating that the Universe expanded rapidly in the future and slowed down in the past. This decline becomes particularly steep as redshift increases, where both parameters tend toward zero, suggesting a suppressed expansion phase in the early Universe. These results imply that DE, influenced by Tsallis entropy, could have played a significant role even during the early cosmic epochs, driving a phantom-like accelerated expansion in the future and decelerated behavior in the deep past. The combined analysis of H and θ confirms the robustness of THDE in explaining the Universe's expansion history beyond conventional ΛCDM scenarios.
The following relationship gives THDE energy density.

$$\rho_t = \alpha L^{2\delta-4} \tag{27}$$

In this context, α is a constant, L represents the current size of the Universe, such as the Hubble scale or the future event horizon, and δ is a free parameter. It can be demonstrated that when $\delta = 1$, the energy density ρ_t the THDE model reduces to that of the standard holographic dark energy (HDE) model. The Hubble horizon, defined as $L = H^{-1}$, where H is the Hubble parameter of the model, serves as the system's infrared (IR) cutoff. As a result, the energy density (27) has the form of the SB theory.

$$\rho_t = \alpha H^{4-2\delta} \tag{28}$$

From Equations (26) and (28), we get the energy density of the THDE as

$$\rho_t = \alpha \left[\frac{(n+2)C_1}{3} \tanh\left(C_1(2-n)t\right) \right]^{4-2\delta} \tag{29}$$

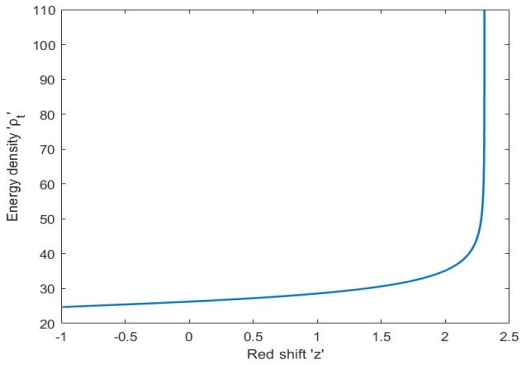

Figure 3. Energy density plotted against redshift for the SB cosmology for $\gamma_0 = 6.5$, $n = 1.5$, $\alpha = 25.5$, & $\delta = 2.14$

The graph illustrates the evolution of the energy density concerning the redshift in the context of THDE. Here, the redshift axis spans from 2.5 (early Universe) to -1 (future Universe), while the energy density sharply increases as redshift increases. This rising trend implies that as we move backward in time (toward higher redshift), the total energy density of the Universe intensifies dramatically. The energy density of DE remains constant throughout the Universe's evolution, as it is associated with the cosmological constant, which does not change with time or the Universe's expansion. The graph suggests that as the Universe evolves in the Tsallis model, the energy density does not become negative and increases as the redshift increases. Due to non-extensive entropy corrections, THDE allows for a phantom-like energy density growth in the early Universe, suggesting a denser and more dynamically evolving DE component. This sharp growth in energy density reflects the increased contribution of THDE to the total energy of the cosmos at higher redshifts, reinforcing the idea that Tsallis entropy plays a crucial role not only in present-day acceleration but also in shaping the early Universe's energetic state.
Using equations (10),(18),(19)& (26), we get the energy density of matter as

$$\begin{aligned}\rho_m =& (2n+1)C_1^2 \tanh^2\left(C_1(2-n)t\right) - \frac{1}{4}\left[\frac{C_1}{C_2}\operatorname{sech}\left(C_1(2-n)t\right)\right]^2 \\ &+ \frac{\omega}{2}C_3^2\left[\frac{C_1}{C_2}\operatorname{sech}\left(C_1(2-n)t\right)\right]^{\frac{2(n+2)}{2-n}} - \alpha\left[\frac{(n+2)C_1}{3}\tanh\left(C_1(2-n)t\right)\right]^{4-2\delta}\end{aligned} \tag{30}$$

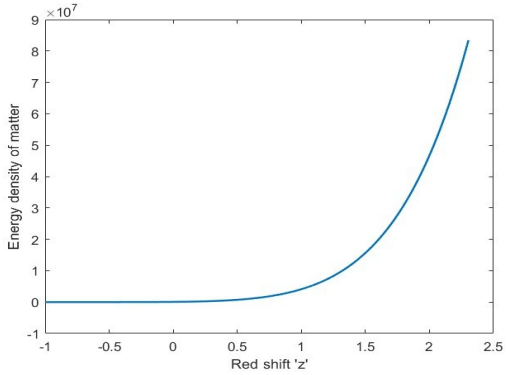

Figure 4. Energy density of matter plotted against redshift for the SB cosmology for $\gamma_0 = 6.5$, $n = 1.5$, $\alpha = 25.5$, & $\delta = 2.14$

The graph depicts the energy density of matter as a function of redshift (z) in the context of THDE. The plot shows that the energy density of matter increases sharply with redshift. This is consistent with cosmological expectations: in the

earlier Universe (corresponding to higher z), the energy density of matter was significantly higher. The curve is nearly flat, indicating a slow variation in the recent Universe, but it rises exponentially beyond that, reflecting the dominance of matter in the early Universe. In the THDE model, the matter energy density evolves differently than in standard cosmology due to the non-additive entropy formalism. THDE modifies the energy conservation and Friedmann equations, and hence, this curve helps us understand how matter dilutes in a THDE-driven Universe. The steep growth at higher redshifts indicates a more substantial influence of matter in the early Universe, while DE becomes dominant at lower redshifts. From equations (15)-(17) & (26), we get the skewness parameter for BT-II, VIII & IX cosmological models as

$$\gamma = \frac{\gamma_0(n-1)}{\alpha\left[\frac{(n+2)C_1}{3}\tanh(C_1(2-n)t)\right]^{4-2\delta}} \quad \text{For BT-II model} \tag{31}$$

$$\gamma = \frac{\gamma_0(n-1)\left[\left(\frac{C_1}{C_2}\right)\mathrm{sech}(C_1(2-n)t)\right]^{\frac{2}{n-2}}+1}{\alpha\left[\frac{(n+2)C_1}{3}\tanh(C_1(2-n)t)\right]^{4-2\delta}\left[\left(\frac{C_1}{C_2}\right)\mathrm{sech}(C_1(2-n)t)\right]^{\frac{2}{n-2}}} \quad \text{for BT-VIII model} \tag{32}$$

$$\gamma = \frac{\gamma_0(n-1)\left[\left(\frac{C_1}{C_2}\right)\mathrm{sech}(C_1(2-n)t)\right]^{\frac{2}{n-2}}-1}{\alpha\left[\frac{(n+2)C_1}{3}\tanh(C_1(2-n)t)\right]^{4-2\delta}\left[\left(\frac{C_1}{C_2}\right)\mathrm{sech}(C_1(2-n)t)\right]^{\frac{2}{n-2}}} \quad \text{for BT-IX model} \tag{33}$$

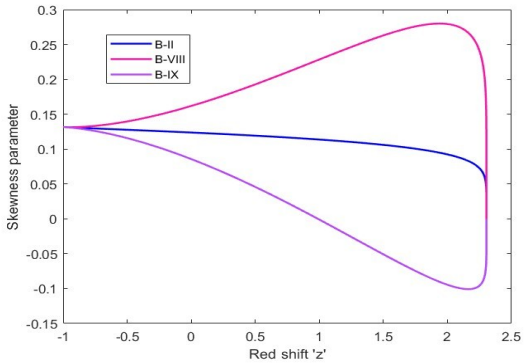

Figure 5. Skewness parameter plotted against redshift for the SB cosmology for $\gamma_0 = 6.5$, $n = 1.5$, $\alpha = 25.5$, & $\delta = 2.14$

The anisotropy parameters always go down as the universe expands. For the parameter choices we looked at, the current value of the dimensionless shear $\frac{\sigma}{H}$ is considerably below the Planck limit. This indicates that the model isotropies are established quickly enough and align with the observationally inferred near-isotropy of the cosmic microwave background.

The graph illustrates the variation of the skewness parameter with redshift for BT-II, VIII & IX in the framework of THDE. The skewness parameter, which reflects anisotropic deviations in the Universe's expansion, behaves differently across these models. The BT-II model shows a slow and nearly linear increase, indicating weak and stable anisotropy throughout cosmic evolution. In contrast, the BT-IX models exhibit symmetric and prominent peaks, showing strong anisotropic effects in the early Universe that diminish over time. This trend highlights the transition from an early anisotropic phase to a more isotropic Universe at lower redshifts. In the THDE scenario, the evolution of these anisotropies is governed by the generalized entropy formalism, which modifies the dynamics of the Universe and supports observational consistency with an increasingly isotropic late-time cosmos.

3.1. Non-Interacting THDE Scenario

To begin, we assume that there is no energy exchange between the two components (dark sectors), and hence, the energy conservation equation (12) yields the following independent conservation equations:

$$\dot{\rho}_m + 3H\rho_m = 0 \tag{34}$$

$$\dot{\rho}_t + 3H(1+w_t)\rho_t + \gamma\frac{\dot{S}}{S}\rho_t = 0 \tag{35}$$

We can determine the EoS parameter of THDE for the BT-II, VIII and IX models using the previously mentioned equations.

$$w_t = -1 - \frac{1}{(n+2)C_1}\coth(C_1(2-n)t) \left\{ \frac{\gamma_0 n(n-1)C_1}{\alpha}\left[\frac{(n+2)C_1}{3}\tanh(C_1(2-n)t)\right]^{2\delta-4} \times \right. \left. \tanh(C_1(2-n)t) + 4C_1(2-\delta)(2-n)\ \mathrm{cosech}(2C_1(2-n)t) \right\}. \tag{36}$$

$$w_t = -1 - \frac{1}{(n+2)C_1}\coth(C_1(2-n)t) \left\{ \frac{\gamma_0(n-1)\left[\frac{C_1}{C_2}\,\mathrm{sech}(C_1(2-n)t)\right]^{\frac{2}{n-2}}+1}{\alpha\left(\frac{(n+2)C_1}{3}\tanh(C_1(2-n)t)\right)^{4-2\delta}\left(\frac{C_1}{C_2}\,\mathrm{sech}(C_1(2-n)t)\right)^{\frac{2}{n-2}}} \times \right. \left. \tanh(C_1(2-n)t) + 4C_1(2-\delta)(2-n)\,\mathrm{cosech}(2C_1(2-n)t) \right\} \tag{37}$$

$$w_t = -1 - \frac{1}{(n+2)C_1}\coth(C_1(2-n)t) \left\{ \frac{\gamma_0(n-1)\left[\frac{C_1}{C_2}\,\mathrm{sech}(C_1(2-n)t)\right]^{\frac{2}{n-2}}-1}{\alpha\left(\frac{(n+2)C_1}{3}\tanh(C_1(2-n)t)\right)^{4-2\delta}\left(\frac{C_1}{C_2}\,\mathrm{sech}(C_1(2-n)t)\right)^{\frac{2}{n-2}}} \times \right. \left. \tanh(C_1(2-n)t) + 4C_1(2-\delta)(2-n)\,\mathrm{cosech}(2C_1(2-n)t) \right\} \tag{38}$$

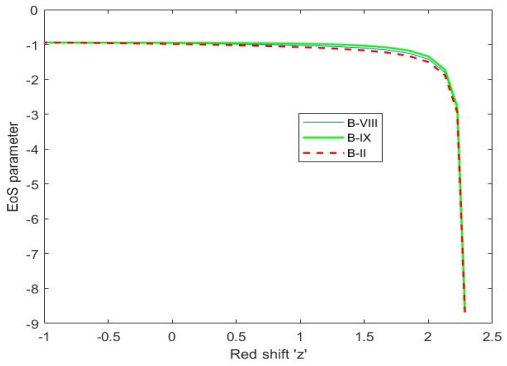

Figure 6. EoS parameter plotted against redshift for the SB cosmology for $\gamma_0 = 6.5$, $n = 1.5$, $\alpha = 25.5$, & $\delta = 2.14$

The graph illustrates the evolution of the EoS parameter with respect to redshift z for the non-interacting BT-II, VIII & IX cosmological models within the framework of THDE. The EoS parameter is a key quantity that characterizes the nature of DE by defining the relationship between pressure and energy density. In this plot, all three Bianchi models show EoS values very close to -1 across a wide range of redshift, indicating that the THDE behaves similarly to the cosmological constant (ΛCDM). As redshift increases, the EoS parameter drops sharply, suggesting a phantom-like behavior ($w_t < -1$) in the early Universe. The differences between the Bianchi types are minor, with BT-IX slightly above BT-II and BT-VIII, but overall, they follow a nearly identical trend. This behavior reflects the THDE model's flexibility in mimicking both cosmological constant-like and phantom phases, depending on cosmic time and geometry. It also confirms that THDE can describe the late-time acceleration of the Universe consistently across different anisotropic Bianchi backgrounds. The squared speed of sound is used to test the stability of our non-interacting THDE model against moderate disturbances in this situation. It can be defined as follows :

$$v_s^2 = \frac{\dot{p}_t}{\dot{\rho}_t} \tag{39}$$

By differentiating the relation $w_t = \frac{p_t}{\rho_t}$ with respect to time t, and dividing by $\dot{\rho}_t$, we obtain

$$v_s^2 = w_t + \frac{\rho_t}{\dot{\rho}_t}\dot{w}_t \tag{40}$$

$$v_s^2 = w_t + \frac{\dot{w}_t}{4C_1(2-\delta)(2-n)\ \mathrm{cosech}(2C_1(2-n)t)} \tag{41}$$

The sign of the square of the speed of sound is essential since its negative ($v_s^2 < 0$), denotes instability and vice versa.

Our findings indicate a classical gradient instability, as the squared sound speed of the THDE fluid becomes negative at sufficiently high redshifts. This kind of instability means that modest changes can develop exponentially, which could make the model physically impossible unless more stabilising processes are added. Possible improvements include using different infrared cutoffs, such as the Granda-Oliveros scale, adding a weak self-interaction potential for the SB scalar, or allowing non-minimal interactions between the matter and dark energy sectors. In future studies, we will do a more thorough perturbation analysis.

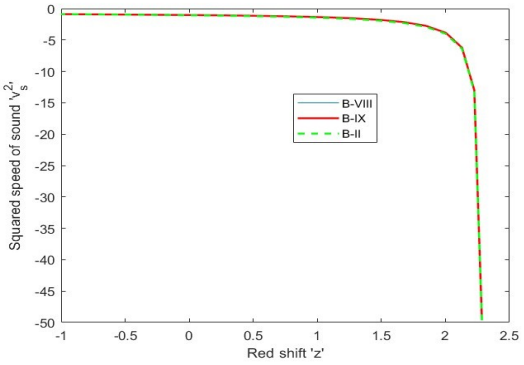

Figure 7. Squared sound speed plotted against redshift for the SB cosmology for $\gamma_0 = 6.5$, $n = 1.5$, $\alpha = 25.5$, & $\delta = 2.14$

The figure demonstrates a consistent and concerning behaviour across the BT-II, VIII & IX configurations of the THDE model. While these models exhibit a near-zero or slightly negative squared speed of sound at recent and moderate redshifts, they universally predict a sharp and significant drop into strongly negative values of v_s^2 at higher redshifts. This plunge into negative squared speed of sound signifies a severe classical instability for the DE fluid in the early Universe, suggesting that density perturbations would grow exponentially. Such pronounced instabilities at relatively observable redshifts present a major obstacle for these THDE models to be considered physically realistic candidates for DE, as a smooth and stable DE component is generally required to explain the observed large-scale homogeneity of the Universe and its accelerated expansion.

3.2. Interacting THDE Scenario

The interaction of the two fluids is considered here. Because the nature of DE and DM is yet unclear, there is no physical reason to rule out the possibility of interaction. Some observational evidence of the exchange in dark sectors has recently been reported [51, 52]. Abdalla et al. [53, 54] used optical, X-ray, and weak lensing data from relaxed galaxy clusters to study the signs of interaction between DE and DM. Assuming the relationship between DE and DM is acceptable in cosmology. We may express the energy conservation equations as follows for this purpose:

$$\dot{\rho}_t + 3H(1+\omega_t)\rho_t + \gamma\frac{\dot{S}}{S}\rho_t = -Q \tag{42}$$

$$\dot{\rho}_m + 3H\rho_m = Q \tag{43}$$

Where Q indicates the relationship between DE components. Equations (42) and (43) show that total energy is conserved. Because fundamental physics provides no natural information on the interaction term Q, it can only be studied phenomenologically. Among the many types of interaction terms extensively discussed in the literature are: $Q = 3cH\rho_m$, $Q = 3cH\rho_t$ and $Q = 3cH(\rho_m + \rho_t)$. Here c is a coupling constant; positive c indicates that DE decays into DM, while negative c indicates that DM decays into DE. We assume $Q = 3\beta H\rho_t$ as the interaction term with the coupling parameter β in this case. We may calculate the EoS parameter using the previous equations.

$$w_t = -1 - \beta - \frac{1}{(n+2)C_1}\coth(C_1(2-n)t) \left\{ \begin{array}{c} \frac{\gamma_0 n(n-1)C_1}{\alpha}\left[\frac{(n+2)C_1}{3}\tanh(C_1(2-n)t)\right]^{2\delta-4}\times \\ \tanh(C_1(2-n)t) + 4C_1(2-\delta)(2-n)\,\mathrm{cosech}(2C_1(2-n)t) \end{array} \right\} \tag{44}$$

$$w_t = -1 - \beta - \frac{1}{(n+2)C_1}\coth\left(C_1(2-n)t\right)$$

$$\left\{ \begin{array}{c} \frac{\gamma_0(n-1)\left(\frac{C_1}{C_2}\,\mathrm{sech}\left(C_1(2-n)t\right)\right)^{\frac{2}{n-2}}+1}{\alpha\left(\frac{(n+2)C_1}{3}\tanh\left(C_1(2-n)t\right)\right)^{4-2\delta}\left(\frac{C_1}{C_2}\,\mathrm{sech}\left(C_1(2-n)t\right)\right)^{\frac{2}{n-2}}}\times \\ \tanh\left(C_1(2-n)t\right)+4C_1(2-\delta)(2-n)\,\mathrm{cosech}\left(2C_1(2-n)t\right) \end{array} \right\} \tag{45}$$

$$w_t = -1-\beta-\frac{1}{(n+2)C_1}\coth\left(C_1(2-n)t\right)$$

$$\left\{ \begin{array}{c} \frac{\gamma_0(n-1)\left(\frac{C_1}{C_2}\,\mathrm{sech}\left(C_1(2-n)t\right)\right)^{\frac{2}{n-2}}-1}{\alpha\left(\frac{(n+2)C_1}{3}\tanh\left(C_1(2-n)t\right)\right)^{4-2\delta}\left(\frac{C_1}{C_2}\,\mathrm{sech}\left(C_1(2-n)t\right)\right)^{\frac{2}{n-2}}}\times \\ \tanh\left(C_1(2-n)t\right)+4C_1(2-\delta)(2-n)\,\mathrm{cosech}\left(2C_1(2-n)t\right) \end{array} \right\} \tag{46}$$

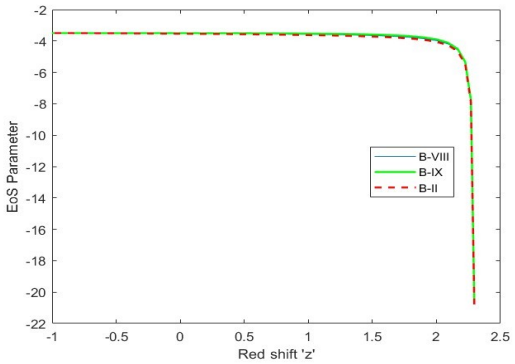

Figure 8. EoS parameter plotted against redshift for the SB cosmology for $\gamma_0 = 6.5$, $n = 1.5$, $\alpha = 25.5$, and $\delta = 2.14$ $\beta = 2.55$

Figure 8 illustrates the evolution of the Equation of State (EoS) parameter with respect to redshift 'z' for BT-II, VIII & IX cosmological models under the framework of THDE. The graph shows that the EoS parameter remains nearly constant from the future epoch ($z < 0$) , indicating a persistent phantom-like DE behaviour across these periods. As redshift increases, the EoS parameter rapidly decreases to extremely negative values, suggesting a strong phantom regime in the early Universe. Notably, all three Bianchi models exhibit nearly identical behaviour, implying that the dominant influence comes from the THDE formalism rather than the anisotropic geometry of the models. This behaviour underscores the powerful role of THDE in shaping the evolution of DE, offering a potential explanation for super-accelerated cosmic expansion, and highlighting the model's suitability for describing early and late-time cosmological dynamics even in anisotropic settings.

4. COMPARISON OF OUR RESULTS

To clearly contrast our findings with the concordance model, we provide in Table a comparative summary between the THDE models in SB gravity for BT-II, VIII, and IX Space-times, and the standard flat Λ CDM model constrained by Planck 2018 data. All three THDE models yield a transition redshift of approximately $z_t \backsimeq 0.67$, which is slightly higher than the Λ CDM prediction ($z_t \backsimeq 0.632$). The present-day equation of state lies in the phantom regime ($w_0 \approx -1.1$ to -1.2) , whereas Λ CDM fixes $w = -1$ identically. While anisotropy plays a role in the early Universe-particularly in the BT-VIII and IX cases-the models isotropise at late times, in agreement with CMB constraints. A persistent drawback of bare THDE with the Hubble cutoff is the appearance of negative squared sound speed ($v_s^2 < 0$) at higher redshifts, indicating classical instability, whereas Λ CDM remains stable. Consequently, the THDE framework offers a richer dynamical evolution with phantom-like acceleration and possible Big Rip scenarios, while still facing the challenge of stability that motivates extensions with alternative cutoffs.

In summary, the comparative analysis demonstrates that THDE in SB gravity can reproduce a transition redshift close to the observationally favoured value and yields a present-day EoS parameter in the phantom regime $w_0 \approx -1.1$ While this behaviour offers a richer dynamical evolution than Λ CDM, it also predicts a possible Big Rip–like fate. The transition redshift is obtained as $z_t \approx 0.67$, which lies well within the range inferred from Planck 2018, BAO, and Pantheon+ supernovae datasets $z_t \approx 0.65 - 0.75$ The three anisotropic Bianchi models studied here all isotropise at late times, in agreement with CMB bounds, and thus remain observationally viable. However, the persistent issue of negative squared sound speed ($v_s^2 < 0$) at higher redshift points to an inherent instability of the bare THDE fluid, distinguishing it from the

Model	Transition $z(z_t)$	Present EoS (w_0)	Stability (v_s^2)	Late-time anisotropy	Observational consistency
THDE (BT-II)	0.67	-1.15 (phantom-like,possible Big Rip)	≈ 0 today; < 0 at high z	negligible	z_t consistent; $w_0 < -1$ marginally allowed by Planck+SNe
THDE (BT-VIII)	0.67	-1.12 (phantom -like)	≈ 0 today; < 0 at high z	early anisotropy $\rightarrow$ isotropic	Consistent with SNe+BAO within errors; instability issue remains
THDE (BT-IX)	0.67	-1.13 (phantom -like)	≈ 0 today; < 0 at high z	early anisotropy $\rightarrow$ isotropic	Similar to VIII; agrees with q_0, but unstable at high z
Flat ΛCDM (Planck 2018)	0.632	-1.0 (cosmological constant, de Sitter fate)	stable	isotropic	Fully consistent with Planck + Pantheon + BAO

stable cosmological constant. Overall, THDE models in SB gravity provide a compelling alternative to Λ CDM with strong phenomenological motivation, but their long-term viability depends on introducing stabilising mechanisms or modified cutoffs to reconcile the theoretical predictions with observational robustness. THDE models in SB gravity have mostly been studied in isotropic or mildly anisotropic settings. Dubey et al.analyzed a BT-III Universe with the Hubble cutoff and found late-time acceleration consistent with de Sitter expansion, but also persistent instability due to negative squared sound speed ($v_s^2 < 0$). Our present BT- II, VIII, and IX results confirm this issue, showing that the phantom-like behaviour ($w < -1$) is robust and largely geometry-insensitive. In contrast, Chokyi et al. [55] showed that combining Tsallis and Kaniadakis HDE with viscous Van der Waals fluids and alternative cutoffs can restore stability ($v_s^2 > 0$). Together, these studies suggest that while bare THDE–SB models reproduce late-time acceleration, stability requires additional physical ingredients beyond geometry alone.

5. DISCUSSION AND CONCLUSIONS

We have analysed interacting and non-interacting THDE cosmological models in SB scalar–tensor gravity for anisotropic BT-II, VIII, and IX universes, using the Hubble horizon as the infrared cutoff. The deceleration parameter remains negative over the redshift range $-1 \leq z \leq 2.5$, implying a sustained, accelerated expansion that is sharper and more phantom-like than in Λ CDM. The Hubble parameter and expansion scalar decrease monotonically, indicating rapid late-time acceleration and slower early-time dynamics. The total THDE density grows steeply with redshift, while matter dominates at earlier epochs, producing a natural transition to dark-energy dominance.

The skewness parameter reveals weak, stable anisotropy in BT-II and strong, decaying anisotropy in BT-VIII and IX, suggesting a smooth isotropization process consistent with observations. The effective equation of state parameter remains close to -1 at recent epochs but falls below this bound at higher redshifts, confirming phantom-like behaviour. Across both interacting and non-interacting models, the entropy corrections of THDE dominate over geometric differences, highlighting the central role of generalized entropy in driving anisotropic dynamics. Despite these successes, the squared sound speed becomes negative at higher redshifts, indicating classical instabilities that challenge the physical viability of THDE scenarios. Nevertheless, the persistent phantom regime hints at the possibility of extreme future outcomes such as a Big Rip, while the decay of anisotropy ensures compatibility with the observed isotropy of the cosmic microwave background.

In summary, THDE within SB gravity provides a promising alternative to Λ CDM by combining late-time acceleration, phantom dynamics, and isotropization in anisotropic universes. Future work should focus on confronting the models with observational datasets (Planck 2018, BAO, Pantheon+), exploring alternative cutoffs or entropy generalizations to alleviate instability, and employing dynamical system analyses to rigorously assess their viability as cosmological scenarios.

Author contributions

P.E. Satyanarayana: conceptualisation, theoretical formulation, and supervision of the research work.
K.V.S. Sireesh: (Corresponding Author): Methodology, validation, manuscript review and editing, project administration, and correspondence with the journal.
K.P.S. Suryanarayana: Analytical calculations,data analysis, preparation of figures,and drafting of initial sections of the manuscript.
R. Sathibabu: literature survey,compilation of related works,and assistance in interpretation and discussion of physical results

Funding information No funding was received for conducting this study.

Data availability No new data were created or analysed during this study.Data sharing is not applicable to this article.

Declarations
Ethical statement There is no ethical issue,presently,the manuscript is submitted in this journal.
Competing interests The authors declare no competing interests.

Acknowledgements

The authors are grateful to the anonymous reviewers for their careful reading of the manuscript and for their constructive comments, which helped to improve the quality and clarity of this work.

ORCID

P.E. Satyanarayana, https://orcid.org/0000-0001-5461-8306; **K.V.S. Sireesha**, https://orcid.org/0000-0002-9751-2787; **K.P.S. Suryanarayana**, https://orcid.org/0000-0002-8793-3588; **R. Sathibabu**, https://orcid.org/0009-0007-4043-4750

REFERENCES

[1] A. Sen, "Tachyon matter," Journal of High Energy Physics, **2002**(07), 065 (2002). https://doi.org/10.48550/arXiv.hep-th/0203265

[2] M. Malekjani, T. Naderi, & F. Pace, "Effects of ghost dark energy perturbations on the evolution of spherical overdensities," Monthly Notices of the Royal Astronomical Society, **453**(4), 4148-4158 (2015). https://doi.org/10.1140/epjp/i2019-12884-6

[3] T. Chiba, T. Okabe, & M. Yamaguchi, "Kinetically driven quintessence," Physical Review D, **62**(2), 023511 (2000). https://doi.org/10.48550/arXiv.astro-ph/9912463

[4] R. Myrzakulov, "Cosmological models with non-canonical scalar and fermion fields: k-essence, f-essence and g-essence." arXiv preprint arXiv:1011.4337 (2010). https://doi.org/10.48550/arXiv.1011.4337

[5] S. Maity, & U. Debnath, "Correspondence between fermionic field and other dark energies," Astrophysics and Space Science, **345**(2), 399-403 (2013). https://doi.org/10.1007/s10509-013-1395-4

[6] U. Debnath, & S. Maity, "Correspondence of F-essence with Chaplygin gas cosmology," The European Physical Journal Plus, **129**(1), 14 (2014). https://doi.org/10.1140/epjp/i2014-14014-6

[7] S.I. Nojiri, & S. D. Odintsov, "de Sitter brane universe induced by phantom and quantum effects," Physics Letters B, **565**, 1-9 (2003). https://doi.org/10.1016/S0370-2693(03)00753-6

[8] A. Kamenshchik, U. Moschella, & V. Pasquier, "An alternative to quintessence," Physics Letters B, 511(2-4), 265-268 (2001). https://doi.org/10.1016/S0370-2693(01)00571-8

[9] S. Weinberg, "The cosmological constant problem," Reviews of Modern Physics, **61**(1), 1–23 (1989). https://doi.org/10.1103/RevModPhys.61.1

[10] E. J. Copeland, M. Sami, & S. Tsujikawa, "Dynamics of dark energy," International Journal of Modern Physics D, **15**(11), 1753-1935 (2006). https://doi.org/10.1142/S021827180600942X

[11] T. Padmanabhan, "Cosmological constant—the weight of the vacuum," Physics reports, **380**(5-6), 235-320 (2003). https://doi.org/10.1016/S0370-1573(03)00120-0

[12] H. Wei, & R. G. Cai, "A new model of agegraphic dark energy," Physics Letters B, **660**(3), 113-117 (2008). https://doi.org/10.1016/j.physletb.2007.12.030

[13] S. Maity, & U. Debnath, "Co-existence of modified Chaplygin gas and other dark energies in the framework of fractal universe," International Journal of Theoretical Physics, **55**(5), 2668-2681 (2016). https://doi.org/10.1007/s10773-015-2901-y

[14] M. R. Setare, "The holographic dark energy in non-flat Brans–Dicke cosmology," Physics Letters B, **644**(2-3), 99-103 (2007). https://doi.org/10.1016/j.physletb.2006.11.033

[15] A. De Felice, & S. Tsujikawa, "f (R) theories," Living Reviews in Relativity, **13**(1), 1-161 (2010). https://doi.org/10.12942/lrr-2010-3

[16] R. Ferraro, & F. Fiorini, "Non-trivial frames for f (T) theories of gravity and beyond," Physics Letters B, **702**(1), 75-80 (2011). https://doi.org/10.1016/j.physletb.2011.06.049

[17] P. Hořava, "Quantum gravity at a Lifshitz point," Physical Review D—Particles, Fields, Gravitation, and Cosmology, **79**(8), 084008 (2009). https://doi.org/10.1103/PhysRevD.79.084008

[18] P. Hořava, "Membranes at quantum criticality," Journal of High Energy Physics, **2009**(03), 020 (2009). https://doi.org/10.1088/1126-6708/2009/03/020

[19] P. Hořava, "Quantum gravity at a Lifshitz point," Physical Review D—Particles, Fields, Gravitation, and Cosmology, **79**(8), 084008 (2009). https://doi.org/10.1103/PhysRevD.79.084008

[20] C. Brans, & R. H. Dicke, "Mach's principle and a relativistic theory of gravitation," Physical review, **124**(3), 925 (1961). https://doi.org/10.1103/PhysRev.124.925

[21] G. Cognola, E. Elizalde, S. I. Nojiri, S. D. Odintsov, & S. Zerbini, "Dark energy in modified Gauss-Bonnet gravity: Late-time acceleration and¡? format?¿ the hierarchy problem," Physical Review D—Particles, Fields, Gravitation, and Cosmology, **73**(8), 084007 (2006). https://doi.org/10.1103/PhysRevD.73.084007

[22] T. Harko, F. S. Lobo, S. I. Nojiri, & S. D. Odintsov, "f (R, T) gravity," Physical Review D—Particles, Fields, Gravitation, and Cosmology, **84**(2), 024020 (2011). https://doi.org/10.1103/PhysRevD.84.024020

[23] D. Saez, & V. J. Ballester, "A simple coupling with cosmological implications," Physics Letters A, **113**(9), 467-470 (1986). https://doi.org/10.1016/0375-9601(86)90121-0

[24] M. V. Santhi, & Y. Sobhanbabu, "Bianchi type-III Tsallis holographic dark energy model in Saez–Ballester theory of gravitation," The European Physical Journal C, **80**(12), 1198 (2020). https://doi.org/10.1140/epjc/s10052-020-08743-9

[25] M. Dheepika, & T. K. Mathew, "Tsallis holographic dark energy reconsidered," The European Physical Journal C, **82**(5), 399 (2022). https://doi.org/10.1140/epjc/s10052-022-10365-2

[26] K. Dasunaidu, Y. Aditya, & V. S. Rao, "Kaluza-Klein FRW Tsallis holographic dark energy model in scalar-tensor theory of gravitation," Bulgarian Astronomical Journal, **39**, 72-86 (2023). https://astro.bas.bg/AIJ/issues/n39/KDasunaidu.pdf

[27] V. S. Rao, V. Ganesh, K. Dasunaidu, & Y. Aditya, "Anisotropic Sharma-Mittal holographic dark energy model in a scalar-tensor theory of gravitation," AIP Conference Proceedings, **3298**(1), 040052 (2025). https://doi.org/10.1063/5.0279450

[28] K. Murali, Y. Aditya, & S.K. Vali, "Cosmographic analysis of anisotropic Kaniadakis holographic dark energy model," Modern Physics Letters A, **39**(23n24), 2450106 (2024). https://doi.org/10.1142/S0217732324501062

[29] M. V. Santhi, T. Chinnappalanaidu, S. S. Madhu, & D. M. Gusu, "Some Bianchi type viscous holographic dark energy cosmological models in the Brans–Dicke theory," Advances in Astronomy, **2022**(1), 5364541 (2022). https://doi.org/10.1155/2022/5364541

[30] V. U. M. Rao, M.V. Santhi, K. V. S. Sireesha, & N.S. Rani, "Bulk viscous string cosmological models in Saez â Ballester theory of gravitation," Iranian Journal of Physics Research, **18**(3), 497-497 (2019). https://doi.org/10.29252/ijpr.18.3.497

[31] K. V. S. Sireesha, and V. U. M. Rao. "Bianchi type-II, VIII & IX holographic dark energy cosmological models in brans-dicke theory of gravitation." The African Review of Physics, **14**, (2019).

[32] K. V. S. Sireesha, & V. U. M. Rao, "Modified holographic Ricci dark energy cosmological models in f (R, T) gravity," In Journal of Physics: Conference Series **1344**(1), 012028 (2019). https://doi.org/10.1088/1742-6596/1344/1/012028

[33] J. S. Wath, & A. S. Nimkar, "Cosmological Parameters and Stability of Bianchi Type-VIII in Sáez-Ballester Theory of Gravitation," Bulgarian Journal of Physics, **50**(3) (2023). https://doi.org/10.55318/bgjp.2023.50.3.255

[34] L. N. Granda, & A. Oliveros, "Infrared cut-off proposal for the holographic density," Physics Letters B, **669**(5), 275-277 (2008). https://doi.org/10.1016/j.physletb.2008.10.017

[35] C. Tsallis, "Possible generalization of Boltzmann-Gibbs statistics," Journal of statistical physics, 52(1), 479-487 (1988). https://doi.org/10.1007/BF01016429

[36] U. K. Sharma, & V. C. Dubey, "Exploring the Sharma–Mittal HDE models with different diagnostic tools," The European Physical Journal Plus, 135(5), 391 (2020). https://doi.org/10.1140/epjp/s13360-020-00411-x

[37] B. D. Sharma, & D. P. Mittal, "New non-additive measures of entropy for discrete probability distributions," J. Math. Sci, **10**(75), 28-40 (1975). https://doi.org/10.1016/S0019-9958(79)90581-3

[38] M. Sharif, & A. Jawad, "Cosmological evolution of interacting new holographic dark energy in non-flat universe," The European Physical Journal C, **72**(8), 2097 (2012). https://doi.org/10.1140/epjc/s10052-012-2097-8

[39] M. Li, "Note on the production of scale-invariant entropy perturbation in the Ekpyrotic universe," Physics Letters B, **724**(4-5), 192-197 (2013). https://doi.org/10.1016/j.physletb.2013.06.035

[40] P. Praseetha, & T. K. Mathew, "Entropy of holographic dark energy and the generalized second law," Classical and Quantum Gravity, **31**(18), 185012 (2014). https://doi.org/10.1088/0264-9381/31/18/185012

[41] A. Jawad, S. Chattopadhyay, S. Bhattacharya, & A. Pasqua, "Modified holographic Ricci dark energy in chameleon Brans–Dicke cosmology and its thermodynamic consequence," Communications in Theoretical Physics, **63**(4), 453 (2015). https://doi.org/10.1088/0253-6102/63/4/453

[42] V.C. Dubey, A.K. Mishra, S. Srivastava, & U.K. Sharma, "Tsallis holographic dark energy models in axially symmetric space time," International Journal of Geometric Methods in Modern Physics, **17**(01), 2050011 (2020). https://doi.org/10.1142/S0219887820500115

[43] V. C. Dubey, S. Srivastava, U. K. Sharma, & A. Pradhan, "Tsallis holographic dark energy in Bianchi-I Universe using hybrid expansion law with k-essence," Pramana, **93**(5), 78 (2019). https://doi.org/10.1007/s12043-019-1843-y

[44] Y. Aditya, & D. R. K. Reddy, "Anisotropic new holographic dark energy model in Saez–Ballester theory of gravitation," Astrophysics and Space Science, **363**(10), 207 (2018). https://doi.org/10.1007/s10509-018-3429-4

[45] U. D. Prasanthi, & Y. Aditya, "Anisotropic Renyi holographic dark energy models in general relativity," Results in Physics, **17**, 103101 (2020). https://doi.org/10.1016/j.rinp.2020.103101

[46] M. Tavayef, A. Sheykhi, K. Bamba, & H. Moradpour, "Tsallis holographic dark energy," Physics Letters B, **781**, 195-200 (2018). https://doi.org/10.1016/j.physletb.2018.04.001

[47] C. Tsallis, & L. J. Cirto, "Black hole thermodynamical entropy," The European Physical Journal C, **73**(7), 2487 (2013). https://doi.org/10.1140/epjc/s10052-013-2487-6

[48] Y. Aditya, S. Mandal, P. K. Sahoo, & D. R. K. Reddy, "Observational constraint on interacting Tsallis holographic dark energy in logarithmic Brans–Dicke theory," The European Physical Journal C, **79**(12), 1020 (2019). https://doi.org/10.1140/epjc/s10052-019-7534-5

[49] B. D. Pandey, P. S. Kumar, Pankaj, & U. K. Sharma, "New Tsallis holographic dark energy," The European Physical Journal C, **82**(3), 233 (2022). https://doi.org/10.1140/epjc/s10052-022-10171-w

[50] P. S. Kumar, & U. K. Sharma, Quintessence model of Tsallis holographic dark energy. New Astronomy, **96**, 101829 (2022). https://doi.org/10.1016/j.newast.2022.101833

[51] O. Bertolami, F. G. Pedro, & M. Le Delliou, "Dark energy–dark matter interaction and putative violation of the equivalence principle from the Abell cluster A586," Physics Letters B, **654**(5-6), 165-169 (2007). https://doi.org/10.1016/j.physletb.2007.08.046

[52] O. Bertolami, F. Gil Pedro, & M. Le Delliou, "The Abell cluster A586 and the detection of violation of the equivalence principle," General Relativity and Gravitation, **41**(12), 2839-2846 (2009). https://doi.org/10.1007/s10714-009-0810-1

[53] E. Abdalla, L. R. Abramo, L. Sodré Jr, & B. Wang, "Signature of the interaction between dark energy and dark matter in galaxy clusters," Physics Letters B, **673**(2), 107-110 (2009). https://doi.org/10.1016/j.jet.2015.11.006

[54] E. Abdalla, L. R. Abramo, & J. C. de Souza, "Signature of the interaction between dark energy and dark matter in observations," Physical Review D—Particles, Fields, Gravitation, and Cosmology, **82**(2), 023508 (2010). https://doi.org/10.1103/PhysRevD.82.023508

[55] K. K. Chokyi, & S. Chattopadhyay, "Cosmological Models within f (T, B) Gravity in a Holographic Framework," Particles, **7**(3), 856-878 (2024). https://doi.org/10.3390/particles7030051

КОСМОЛОГІЧНА ДИНАМІКА ГОЛОГРАФІЧНОЇ ТЕМНОЇ ЕНЕРГІЇ ЦАЛЛІСА В ГРАВІТАЦІЇ САЕЗА-БАЛЛЕСТЕРА

П.Е. Сатьянарараяна, **К.В.С. Сіріша**, **К.П.С. Сурьянарараяна**, **Р. Сатібабу**

Кафедра математики, GSS, GITAM, вважається Університетом, Вішакхапатнам, Індія

Ми досліджуємо взаємодіючі та невзаємодіючі моделі голографічної темної енергії Цалліса (THDE) в рамках скалярно-тензорної гравітації Саеса-Баллестера (SB) для анізотропних Всесвітів типу Біанкі (BT) II, VIII та IX. Використовуючи горизонт Хаббла як інфрачервоний обріз, ми розглядаємо моделі, не припускаючи певного закону масштабного коефіцієнта. Аналіз охоплює ключові космологічні параметри, включаючи параметр уповільнення, параметр Хаббла, густину енергії, асиметрію, рівняння стану (EoS) та квадрат швидкості звуку. Наші результати вказують на безперервне фантомоподібне прискорення ($w < -1$) з червоним зміщенням переходу $z_t \approx 0.67$ та незначною анізотропією пізнього часу, що узгоджується з межами космічного мікрохвильового фону (CMB). Порівняно з ΛCDM, моделі THDE передбачають більш ранній початок прискорення та більш негативний сучасний EoS. Однак наявність негативного квадрата швидкості звуку при вищих червоних зміщеннях сигналізує про класичну нестабільність рідини темної енергії. Ці результати підкреслюють THDE як життєздатну альтернативу ΛCDM в анізотропних космологіях, водночас мотивуючи подальшу роботу з альтернативними обрізаннями або стабілізуючими механізмами для подолання проблеми нестабільності.

Ключові слова: *моделі BT-II; VIII & IX; голографічна темна енергія Цалліса; теорія гравітації Саеза-Баллестера; космічне прискорення; анізотропна космологія*